Head Impact Modeling to Support a Rotational Combat Helmet Drop Test

Ryan Terpsma, MS[*]; Rika Wright Carlsen, PhD*[†]; Ron Szalkowski, MEng*[‡]; Sushant Malave, MS*[‡]; Alice Lux Fawzi, BSE*[§]; Christian Franck, PhD*[‖]; Chad Hovey, PhD*[*]

ABSTRACT

Introduction:

The Advanced Combat Helmet (ACH) military specification (mil-spec) provides blunt impact acceleration criteria that must be met before use by the U.S. warfighter. The specification, which requires a helmeted magnesium Department of Transportation (DOT) headform to be dropped onto a steel hemispherical target, results in a translational headform impact response. Relative to translations, rotations of the head generate higher brain tissue strains. Excessive strain has been implicated as a mechanical stimulus leading to traumatic brain injury (TBI). We hypothesized that the linear constrained drop test method of the ACH specification underreports the potential for TBI.

Materials and Methods:

To establish a baseline of translational acceleration time histories, we conducted linear constrained drop tests based on the ACH specification and then performed simulations of the same to verify agreement between experiment and simulation. We then produced a high-fidelity human head digital twin and verified that biological tissue responses matched experimental results. Next, we altered the ACH experimental configuration to use a helmeted Hybrid III headform, a freefall cradle, and an inclined anvil target. This new, modified configuration allowed both a translational and a rotational headform response. We applied this experimental rotation response to the skull of our human digital twin and compared brain deformation relative to the translational baseline.

Results:

The modified configuration produced brain strains that were 4.3 times the brain strains from the linear constrained configuration.

Conclusions:

We provide a scientific basis to motivate revision of the ACH mil-spec to include a rotational component, which would enhance the test's relevance to TBI arising from severe head impacts.

INTRODUCTION

Human blast exposure can lead to serious and life-threatening injuries, typically classified as primary, arising from the blast wave, and targeting the lungs, middle ear, and brain; secondary, caused from flying debris; tertiary, resulting in blunt impact of the body with its environment; and quaternary, resulting in all other sequelae. In this cascade of potential injuries, blunt impact on the head remains a primary concern, given the critical nature of the brain. In addition, blunt impact environments without blast precursors, such as motorized vehicle collisions, falls from height, and airborne operations during aircraft exit, descent, and parachute landing, expose the warfighter to the risk of head injury.[1] The warfighter's helmet is the main method for head protection, yet much remains to be learned about how well the helmet actually protects the brain.

The Advanced Combat Helmet (ACH) must pass military-specification (mil-spec) testing that prescribes a blunt impact acceleration limit. This specification requires a helmeted magnesium (Mg) Department of Transportation (DOT) headform to be dropped vertically, with an impact speed of 3.1 m/s (10 ft/s), onto a steel, hemispherical target.[1–3] The pass/fail criteria are based on translational acceleration (150 G) alone, absent from any rotational component. This translational acceleration injury risk assessment is based on the Wayne State Tolerance Curve.[4] Without a rotational component, the specification's injury risk application is limited to skull fracture and hematomas (subdural, subarachnoid). There is a growing body of evidence that suggests rotational head motions, rather than translational motions, are more relevant when assessing the risk of traumatic brain injury (TBI), in particular diffuse axonal injury (DAI).[5–9] As a result, there is a critical need to assess brain injury potential arising from the linear constrained configuration of the ACH mil-spec and from modified configurations that induce head rotation to

[*]Terminal Ballistics Technology Department 5421, Sandia National Laboratories, Albuquerque, NM 87185, USA

[†]Department of Engineering, Robert Morris University, Moon Township, PA 15108, USA

[‡]Team Wendy LLC, Cleveland, OH 44110, USA

[§]School of Engineering, Brown University, Providence, RI 02912, USA

[‖]Department of Mechanical Engineering, University of Wisconsin-Madison, Madison, WI 53706, USA

Meetings at which paper was presented: Military Health System Research Symposium (MHSRS), Kissimmee, FL, Aug. 19-22, 2019 (Poster).

doi:https://doi.org/10.1093/milmed/usab374

ascertain whether helmet testing standards should be updated to include a rotational component.

The inclusion of rotation not only results in head motions that are closer to most real world and combat theater impacts (e.g., such as occur in tertiary blast exposure or direct blunt impact) but also allows for a more complete risk assessment of TBI. This enhanced scope arises because impacts that cause only a translational head response result in less brain strain than impacts that cause rotation.[5] Larger strains are produced from rotational head motions since rotation induces shear deformations. The brain can more easily undergo shear (volume preserving, isochoric) deformations than volumetric (volume changing, dilitational) deformations since its shear modulus is 5-6 orders of magnitude lower than its bulk modulus.[10] As a result of these large shear deformations, DAI can result, which is widespread damage to neuronal axons and one of the main pathological features of TBI.[6] Diffuse axonal injury has been shown to be dependent on both the tissue strain and strain rate, with larger strains and strain rates correlating to an increased risk of DAI.[9,11–13] Combat helmets that pass the ACH mil-spec with the linear constrained configuration may not protect against this common form of TBI.

To inform a revision of the ACH mil-spec such that it accounts for strain and strain rate driven injury, it is critical to understand the relationship between rotational head kinematics and the resulting tissue strains and strain rates that develop within the brain. Finite element (FE) head models can provide valuable insight into the brain deformation response for a given impact condition.[14] It has been shown that the peak tissue strains and strain rates that develop in the brain are dependent on both the magnitude of the peak angular acceleration and peak angular velocity of the head.[15] By characterizing the tissue strains and strain rates that result from a head impact through FE head models, we can begin to guide the development of new helmet testing methods that include a rotational component and provide a better assessment of brain injury risk.

In this study, we explore an alternative approach for testing the ACH that honors the acceleration-based traditions of the existing specification but, importantly, modifies the target anvil configuration to produce rotational head motions. The linear constrained configuration of the ACH mil-spec has an implicit assumption that external impacts on the helmet result in a force application that has near-perfect alignment with the head's center of gravity (CG). Such an impact will likely elicit minimal brain strain because the impact imparts minimal-to-no head rotation. Moreover, this simplifying configuration is an unrealistic assumption on the nature of real-world impacts encountered by the U.S. warfighter in the field. For an arbitrary impact on the helmeted head, the CG-aligned event is a very rare and special case. In conceivable real-world impacts, non-alignment will be present. Through a simple modification of the target anvil configuration that introduces a non-alignment of the impact force with the head's CG, we can elicit a rotational head motion in our test method.

In the following sections of this paper, we describe the methodology of this study, which utilizes physical head impact tests and characterizes the brain deformation response from each test through an FE analysis. The brain strains and strain rates resulting from each testing configuration are presented, and the significance of these results toward the improvement of the ACH mil-spec is discussed.

METHODS

Our methodology followed a sequence of experimental tests, simulation verification, and analysis of brain tissue deformation. Starting with the linear constrained configuration, we established an experimental baseline. We conducted physical tests of an ACH-fitted Mg DOT headform subjected to a crown impact, which produced repeatable headform acceleration time histories (Fig. 2). Two anvils were considered: (1) the hemispherical target of the linear constrained configuration (Fig. 1A), and (2) an inclined anvil (flat surface inclined 45° from horizontal, Fig. 1B). We refer to these two variants as the "linear constrained configuration" and the "modified configuration," respectively. Our modified configuration replaced the DOT headform of the ACH mil-spec with a Hybrid III headform to adequately secure it to the ACH, particularly during the post-impact rotational response. In the former test, a linear constrained drop arm was used. In the latter test, a cradle was used to allow the helmeted headform to have freefall impact with the anvil. Apart from the headform, cradle, and anvil modifications, all other test variables were held constant across the two tests, including the 3.1 m/s (10 ft/s) impact speed specified in the ACH standard. Headform CG acceleration time histories, both three-axis translational and three-axis rotational, were obtained with a CADEX data acquisition system (CADEX Inc., Quebec, Canada). Raw acceleration time history data were post-processed with a four-pole Butterworth filter with the low-pass cutoff frequency of 1,650 Hz.

Simulations of the linear constrained configuration were then performed to verify the computational methodology. All models used for this study were built on a simulation framework that has been previously described and verified.[16,17] Our technical report[17] contains comprehensive details on the geometric models, constitutive models, and complete Sierra Solid Mechanics solver[18] input decks that can be used to reproduce the numerical results produced herein. The salient simulation methodology is as follows: We created a half-symmetry FE model of the DOT, ACH, and hemispherical anvil. Then, we applied homogeneous displacement boundary conditions to the out-of-plane (left-to-right) axis. Although the DOT model had left-to-right symmetry, allowing faster running simulations to be exploited, the human head model, described below, lacked perfect symmetry and thus required a full 3D simulation. The helmeted DOT model was allowed to fall vertically onto the anvil, impacting at the crown location with a speed of 3.1 m/s (10 ft/s). For the DOT simulations, we processed

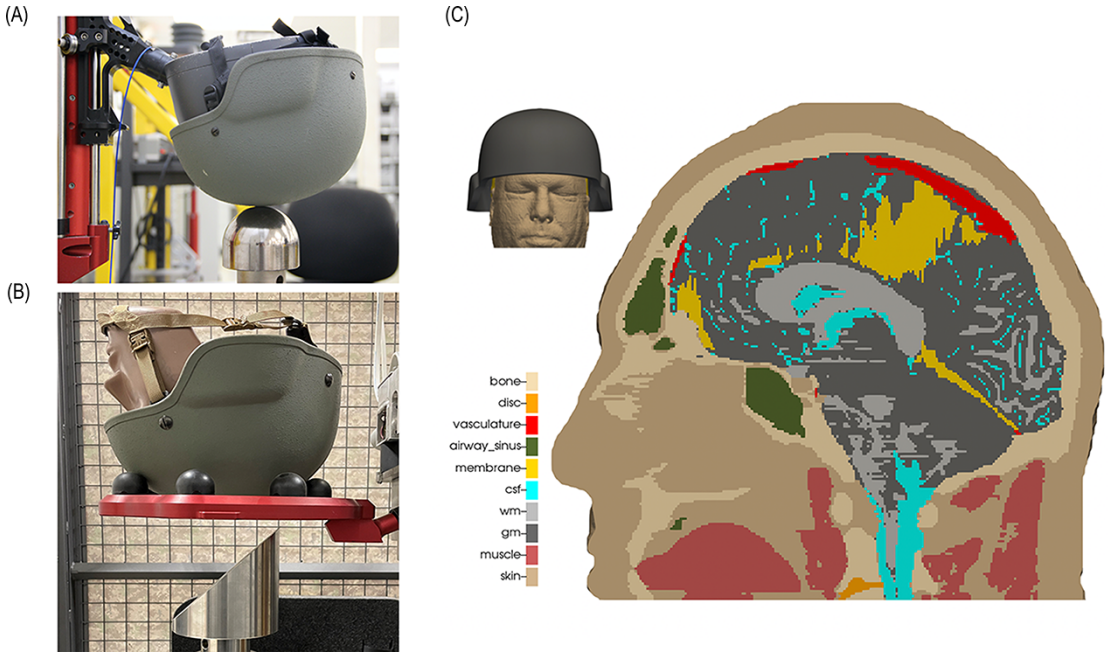

FIGURE 1. Experimental setup, side view, of (A) linear constrained configuration and (B) modified configuration. (C) The three-dimensional human head digital twin mid-sagittal view, illustrating biological tissues modeled in the simulations, with model shown helmeted for context on the small inset image. The human head model in (C) was used to simulate the experimental head impacts and to predict brain strain and strain rate resulting from the configurations shown in (A) and (B).

CG accelerations and compared them to the DOT CG accelerations from our experiments with the linear constrained configuration.

After the numerical digital twin of the linear constrained configuration test was established, we substituted the numerical DOT with a human head digital twin. The acceleration time histories at the human head CG location from the simulations were compared to the CG accelerations recorded in our experiments. The human head digital twin used in this study has been used extensively for blast, blunt, and ballistic military applications and is described in detail in past publications.[19–23] In summary, the human digital twin (Fig. 1C) used for the present investigation consisted of an FE model composed of 4,631,316 three-dimensional hexagonal elements of 1-mm^3 median element size and included skin, muscle, bone, gray matter (GM), white matter (WM), cerebrospinal fluid (CSF), membranes, vasculature, intravertebral discs, airway, and sinus.

The acceleration data (Fig. 2) acquired from the Hybrid III headform in the modified configuration experiments were time-integrated to obtain velocity time histories, both translational and rotational, to use as time-dependent boundary conditions on the skull of the human digital twin, simulating the helmeted human head subjected to the modified configuration impact. For all simulations, the WM and GM Green-Lagrange strain and strain rates were calculated. From these two tensors, the maximum principal strain (MPS) and maximum principal strain rate (MPSR) were tracked for each FE composing the WM (504,505 elements) and GM (790,102 elements). We followed the brain's MPS and MPSR values throughout the impact events and, for each simulation, identified the time when the MPS reached its maximum critical value, which was used in the third and final step of our methodology, described next.

We used brain tissue deformation, adopted widely in biomechanics research[8,9,24,25] to provide a context of brain injury potential to the human digital twin from the linear constrained configuration as well as the modified configuration. At the brain MPS critical times, we plotted strain and strain rate (Fig. 3) in the format of a bivariate distribution, allowing strain and strain rate effects to be viewed independently of each other. The potential clinical significance of these brain strain and strain rate data were assessed using a newly proposed but preliminary injury risk criterion based on the results of an in vitro model of neuronal injury.[11] This cellular-based mild traumatic brain injury (cbmTBI) criterion utilizes both the strain and strain rate of brain tissue to account for the tensile stretch and rate of stretch that occurs throughout the brain as a result of blunt impact to the head. Neuronal strain and strain rate of the cbmTBI criterion, indicated as the "cell death" curve in Figure 3, provide a potential injury threshold for the human brain exposed to both the linear constrained and modified configurations. Strains and strain rates that exceed this threshold (i.e., located to the top and right of the "cell death" curve in Fig. 3) correspond to permanent cellular injury.

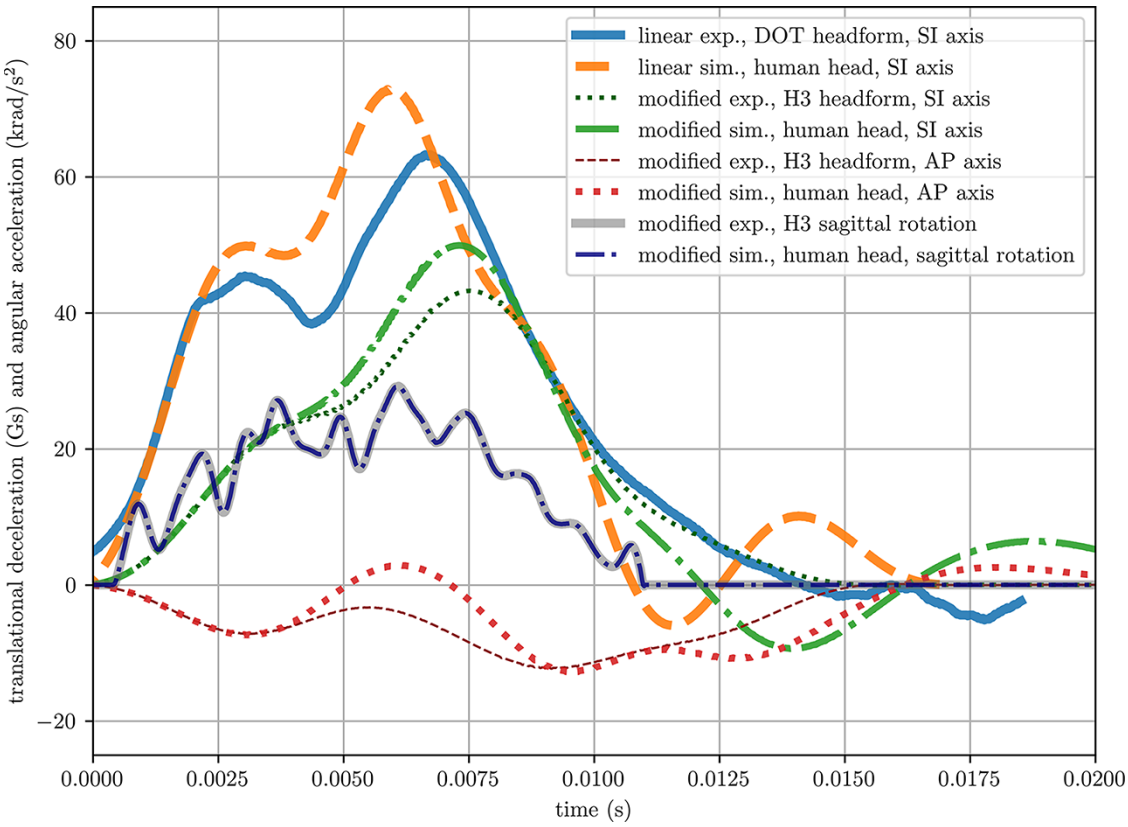

FIGURE 2. Translational deceleration time histories in the superior-inferior (SI) direction are shown by the bold solid curve for the linear constrained experiment (Department of Transportation headform) and by the bold dashed curve for the linear constrained simulation (human head). Translational decelerations in the anterior-posterior (AP) and superior-inferior (SI) direction are shown by the dot/dash-dot and dash/dot curves, respectively, for the modified experiment (Hybrid III or H3 headform) and simulation (human head). The angular head acceleration about the sagittal plane is shown to be the same for the modified experiment (solid curve) and simulation (dash-dot curve).

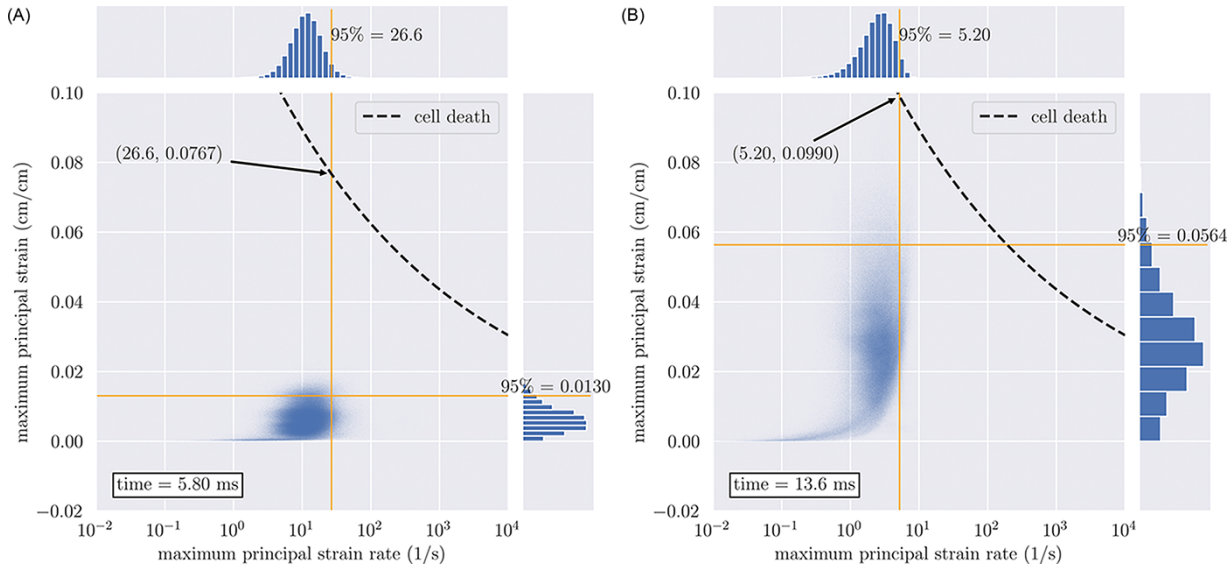

FIGURE 3. Population of white and gray matter finite element tensile maximum principal strain (MPS) and maximum principal strain rate (MPSR) for the (A) linear constrained configuration and (B) modified configuration when the 95th percentile strain has reached a maximum in each of the respective simulations.

RESULTS

As shown in Figure 2, the linear constrained configuration experiments reliably produced peak headform CG accelerations of ∼60-Gs. Relative to this baseline, simulation of the linear constrained experiments with the human head digital twin produced CG acceleration, measured along the head's superior-inferior (SI) axis, with a larger peak (∼70-Gs). Simulation of the human head digital twin impacting the inclined anvil of the modified configuration produced lower vertical SI-axis accelerations (∼50-Gs) but resulted in anterior-posterior (AP) axis accelerations (non-existent for the linear constrained configuration) on the order of 10-Gs. For vertical accelerations, increasing peaks corresponded to shortened pulse durations, with first return-to-zero trace crossings at about 14 ms for the linear constrained experiments, just under 11 ms for the linear constrained simulation, and about 12 ms for the modified cases.

The linear constrained configuration resulted in a single vertical (SI-axis) reaction force on the helmeted headform. In contrast, the inclined anvil of the modified configuration generated reaction forces that caused the helmeted headform to have vertical and anterior (AP-axis) rebounds, with post-impact rotation in the sagittal plane. Headform angular velocity was just over 17 rad/s, with onset duration of ∼10 ms. Over this time interval, peak angular acceleration reached nearly 30 krad/s^2 (Fig. 2). Total headform angular motion during the 10 ms impact was nearly 6°.

Figure 3 shows point clouds and population histograms of strain and strain rate for every FE of the GM and WM for the linear constrained and modified configurations, respectively, at the critical MPS time described in the Methods section. The 95th percentile values of strain and strain rate indicated are commonly used as a conservative estimate when reporting maximum values from numerical simulations.[14] For the linear constrained configuration, the 95th percentile maximum strain was found to be 1.30e-02 (Fig. 3A). For the modified configuration, the 95th percentile maximum strain was found to be 5.64e-02 (Fig. 3B). The modified configuration thus caused a strain magnitude increase of 4.3x, relative to the constrained configuration baseline. At these same simulation times, the modified versus linear constrained strain rate ratio was 5.20/s to 26.6/s, or 0.2x. Thus, the modified configuration, relative to the linear constrained configuration, resulted in increased strain but decreased strain rates.

Figure 4 shows critical MPS for sequential axial sections of the head, for both the linear constrained (left images) and modified (right images) configuration. Paired images in each panel show that the modified configuration causes larger MPS than the linear constrained configuration. Furthermore, Figures 3 and 4 show that the modified configuration results in a wider distribution of strain values throughout the brain as compared to the linear constrained configuration. In both test configurations, the largest brain strains occur at the periphery, where the GM sits adjacent to the CSF/membrane interfaces and the interior of the skull. Elevated GM strain is also observed near the brainstem.

DISCUSSION

We have attempted to justify our main hypothesis: the linear constrained configuration of the ACH mil-spec likely underreports potential for TBI. With the same impact speed of 3.1 m/s (10 ft/s), a modified configuration that elicits post-impact head rotation greatly increased brain strain. Analysis of this comparison, consistent with the growing body of evidence that emphasizes head rotations over translations for TBI risk assessment, suggests that helmet testing standards should include a rotational component.

Our exploration of the mil-spec test demonstrates the need for new helmet liners that mitigate head rotation. For the linear constrained configuration, our results provide a baseline of peak brain strain and strain rate, which new liners must not exceed. For the modified configuration, our results not only demonstrate the limitations of the current helmet liner to mitigate rotation but also provide a known upper bound of peak strain and strain rate, which future rotation-mitigating helmet liners must decrease.

Relative to the linear constrained configuration, the modified configuration caused a strain magnitude increase of 4.3x, the basis to support a specification update. Although the linear constrained configuration may help limit injury risk to skull fracture, it does not equally well predict propensity for rotation-induced brain injury. More work is needed to identify the full scope of real-world, off-axis (non-CG-aligned) helmeted head impacts and to identify the expected brain strain operational envelope present in combat environments.

The rationale to support a specification update stems from the underlying physiology of the brain tissue, which is strongly susceptible to more shear deformation compared to bulk deformation. Shear deformation of the brain, secondary to blunt impact, is more easily achieved through head rotation than through head translation. Thus, a helmet, with the incontrovertible intent of head protection, should be designed to meet a specification that tests head rotations, a particularly deleterious outcome of off-axis head impact.

When the deformation, measured through strain, and the deformation temporal onset, measured through strain rate, is sufficient to exceed the normative physiological thresholds, tissue injury can result.[9] The point clouds (Fig. 3) demonstrate the brain tissue is more at risk for potential cell death by way of excessive strain than by the excessive strain rate. For the linear constrained configuration (Fig. 3A), the distance from the 95th percentile strain, 1.30e-02, to the cell death curve intercept, ∼7.67e-02, is only 6.37e-02. For the modified configuration (Fig. 3B), the distance from the 95th percentile strain, 5.64e-02, to the cell death intercept, ∼9.90e-02, is only 4.26e-02. In contrast to strain, the strain rate 95th percentiles fall far from the cell death curve. The linear constrained

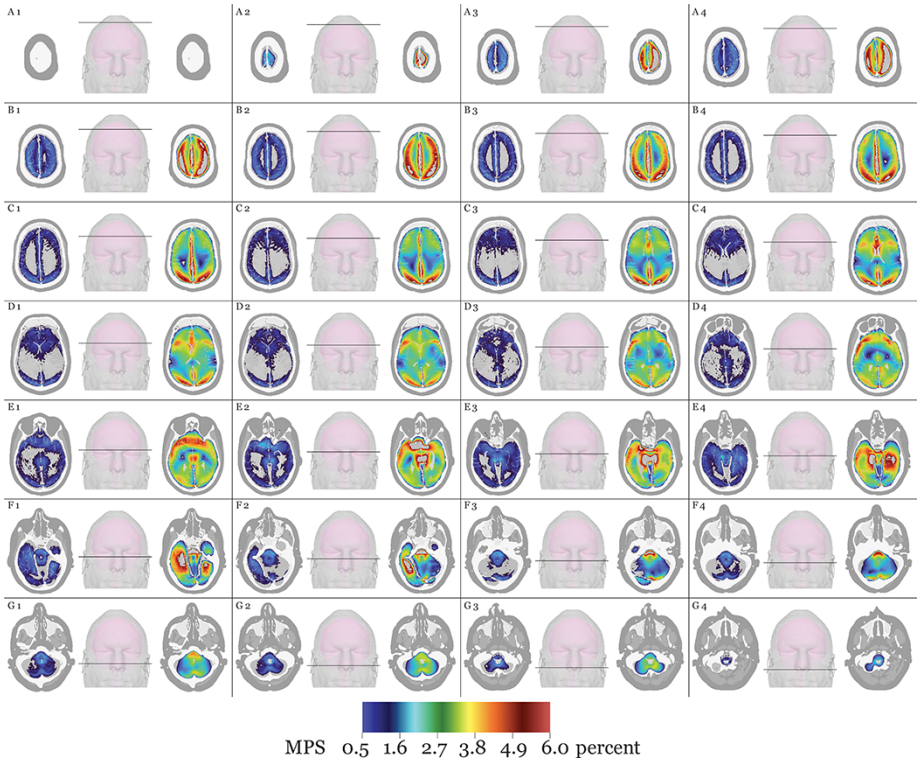

FIGURE 4. Sequence of maximum principal strain (MPS) for axial sections of the head. In each panel (A1 through G4), the center image shows the axial plane elevation, superior-to-inferior. The left image shows the linear constrained configuration results at the given axial plane elevation, and the right image shows the modified configuration results. A comparison between the right and left images shows that the MPS is larger in magnitude for the modified configuration as compared to the linear constrained configuration.

configuration is more than 2.5 orders of magnitude, and the modified configuration is about 1.5 orders of magnitude away from the cell death intercept. Thus, for the two anvil configurations investigated here, strain magnitudes were more critical than strain rates for potential injury. Although the concept that the brain tissue, to remain shielded from injury, should neither be stretched too far nor too fast, the relative contribution to injury from strain versus strain rate is not resolved and remains an active area of research.[12,26]

Compared to the linear constrained configuration, the modified configuration produced elevated brain strains in the human digital twin. These data, mapped to the suggested cbmTBI criterion, demonstrate blunt impacts that cause rotation and translation, rather than just translation alone, have enhanced potential to cause brain injury. These data suggest rotation may play a critical and perhaps dominant role in brain injury causation. There is broad consensus that head rotations are critical to the assessment of brain injury risk.[5–9] To our knowledge, this is the first study that has applied an injury criterion that is based on both tissue strain and strain rate to the ACH mil-spec with a high-fidelity digital human head surrogate in an effort to motivate an update that includes rotation. Although the cbmTBI threshold values used in this study are based on preliminary findings,[11] excluding the cell death curve in Figure 3, all results shown in Figures 2-4 are independent of the cbmTBI criterion and thus useable with alternative injury criteria. Although several other tissue-based injury criteria exist,[9,13,24,25,27–29] this overarching principle persists: as brain tissue deformation increases beyond normal physiological values, so does the probability of injury. Critical values and thresholds are often included to assign increasing deformation magnitudes to increasing injury severity.

Although studies have simulated the acceleration responses based on the ACH mil-spec,[1,30] they used only a DOT headform, not a human model, and examined translations alone, not translations and rotations. Other studies[31] have used a detailed human head model but focused on effects of helmet shell stiffness and helmet-to-skull coupling, finding that the skull, when struck by the helmet shell, resulted in bone fracture. Another recent study by Begonia et al.[32] studied a modified testing configuration that induced rotational head motions by using two dummy neck variants, a Hybrid III and a EuroSID-2, attached to a National Operating Committee for Standards on Athletic Equipment headform. Our modified configuration, in contrast, utilized a simpler setup of a Hybrid III headform without a neck and required only a modification to the anvil target. Both our study and the Begonia study support the conclusion that testing methods that include a rotational component may be more suitable for evaluating the risk of diffuse brain injuries.

Translational acceleration, absent from any other metric, is not a good predictor of brain injury potential. Peak vertical G-loading for the linear constrained configuration exceeded that of the modified configuration since the latter was able to deflect the helmeted head laterally and generate rotations on rebound. This result is expected. For the modified configuration, not all of the inbound translational kinetic energy rebounds as translational kinetic energy, as in the linear constrained configuration case. Rather, the inbound kinetic energy gets transformed, post-collision, into rebounded translational kinetic energy and newly onset rotational kinetic energy. The modified configuration produced lower impact acceleration yet elevated strains, relative to the baseline configuration.

The cause of this outcome can be attributed to the brain's nearly incompressible nature, a consequence of the brain's composition by weight to be predominantly water (77% to 78%).[33] The brain has significant predisposition to undergo shear deformation rather than volumetric deformation. The bulk modulus (K) of the brain exceeds its initial and long-term shear moduli (G_0 and G_∞) by $\sim$ 5-6 orders of magnitude. Bulk modulus is typically measured in GPa (1E9 Pa), whereas shear moduli are typically measured in kPa (1E3 Pa) or 10s of kPa (1E4 Pa). A consequence of the bulk-to-shear disparity is the generalization that rotational head motion, relative to translational head motion, causes greater brain deformation through shear.[10]

Figure 4 shows axial sections of brain strain, comparing the maximum values observed in the two configurations investigated here. Generally, the modified configuration showed elevated strain levels throughout the brain. High values of brain strain appeared near the periphery of the brain, where the GM sits adjacent to the CSF and the interior of the skull. Elevated GM strain also appeared near the interface with the membranes. Less detectable was any effect from the GM-WM interface. This result was expected, since our numerical model for GM and WM differed in shear response only; bulk constitutive response was the same for both materials.[17] This result also indicated that shear constitutive disparities between GM and skull largely saturated any relatively small disparities between GM and WM, at the presently shown strain thresholds.

The present work has important limitations, falling into three broad categories of influence: head kinematics, brain constitutive model, and brain response metric.

First, we compared only two distinct blunt impact configurations: an impact directed toward the crown of a helmeted head and an angled impact posterior to the crown. The ACH military-specification uses seven impact locations, which includes the crown.[1,2] Head impact location and direction is believed to be an important variable influencing the potential for TBI.[34–36] Moreover, our rotational case considered only sagittal rotation. Other studies have shown injury outcomes are dependent on the rotation axis.[6,7,37,38] Our rotational case also utilized a simplified setup of a Hybrid III head without a neck, and while this methodology has been employed in other test methodologies for recreational sports helmets, the specific interaction of the neck should be considered in future studies of combat helmets.

Second, the brain of our 3D human digital twin is isotropic, lacking the anisotropy of the 2D models developed by our team.[39] Because it is such a profound feature of the WM tracts,[40] anisotropy should be included in our future 3D model.

Third, we focused on MPS since this provided a direct comparison to a potential cellular-mild-TBI threshold.[11] Although MPS is frequently reported as a brain injury explanatory variable, other reported metrics include third principal strain, shear strain, volumetric strain rate measure, cumulative strain damage measure, and combinations thereof. There is not yet broad consensus as to which explanatory variable (or variables) best predict(s) TBI.[12,26,38]

CONCLUSION

We have shown that a modified configuration that generated rotations is more deleterious to the brain than the translational impact arising from the ACH mil-spec. Brain deformation, and not acceleration alone, should be used as an explanatory variable for brain injury risk potential. As shown by our comparison of two configurations, the inclined anvil configuration caused lower accelerations and higher deformations than the mil-spec configuration, illustrating the need to distinguish between translational and rotational variables.

The ACH mil-spec deserves a renewed evaluation for its relevance to the risk assessment of head injury, secondary to blunt impact. Without a rotational component, the ACH mil-spec is incapable of fully predicting brain injury. A modification that includes a rotational component would provide updated relevance to prediction and risk assessment of brain injury resulting from blunt impacts.

ACKNOWLEDGMENTS

The authors gratefully acknowledge Dr. Timothy Bentley, Office of Naval Research. The authors also thank the anonymous reviews for their insights and comments, which improved the quality of the manuscript.

FUNDING

This work was supported by the Office of Naval Research (Dr. Timothy Bentley) under PANTHER grant N0001418IP00054 and N000141812494.

CONFLICT OF INTEREST STATEMENT

None declared.

AUTHOR CONTRIBUTION

R.S. and S.M. led and performed the experiments, all other others contributed technical expertise to the design and results interpretation of the experiments. C.H. and R.T. led and performed the simulations, all other authors contributed technical expertise to the design and results interpretation of the simulations. All authors contributed to the development and production of the manuscript.

REFERENCES

1. McEntire BJ, Whitley P: *Blunt Impact Performance Characteristics of the Advanced Combat Helmet and the Paratrooper and Infantry Personnel Armor System for Ground Troops Helmet*. Army Aeromedical Research Lab; 2005.
2. Stone R: *Advanced Combat Helmet Technical Assessment*. Office of the Inspector General (Department of Defense); 2013.
3. National Research Council: Review of Department of Defense Test Protocols for Combat Helmets, 2014. Published online.
4. Hodgson VR, Thomas LM: Comparison of head acceleration injury indices in cadaver skull fracture. SAE Trans 1971; 80(4): 2894–902. Published online.
5. Kleiven S: Why most traumatic brain injuries are not caused by linear acceleration but skull fractures are. Front Bioeng Biotechnol 2013; 1: 15.
6. Gennarelli TA, Thibault LE, Adams JH, Graham DI, Thompson CJ, Marcincin RP: Diffuse axonal injury and traumatic coma in the primate. Ann Neurol Off J Am Neurol Assoc Child Neurol Soc 1982; 12(6): 564–74.
7. Rowson S, Duma SM, Beckwith JG, et al: Rotational head kinematics in football impacts: an injury risk function for concussion. Ann Biomed Eng 2012; 40(1): 1–13.
8. Takhounts EG, Hasija V, Ridella SA, Rowson S, Duma SM: Kinematic rotational brain injury criterion (BRIC). In: Proceedings of the 22nd Enhanced Safety of Vehicles Conference. Paper. Washington, DC, USA; 2011: 1–10.
9. Hajiaghamemar M, Seidi M, Margulies SS: Head rotational kinematics, tissue deformations, and their relationships to the acute traumatic axonal injury. J Biomech Eng 2020; 142(3): 031006–1–13.
10. Zhang L, Yang KH, King AI: Comparison of brain responses between frontal and lateral impacts by finite element modeling. J Neurotrauma 2001; 18(1): 21–30.
11. Summey LA: Development of a simple shear impact device for evaluating cellular traumatic brain injury. Published online 2020.
12. Bar-Kochba E, Scimone MT, Estrada JB, Franck C: Strain and rate-dependent neuronal injury in a 3D in vitro compression model of traumatic brain injury. Sci Rep 2016; 6(1): 1–11.
13. Morrison B, Cater HL, Wang CC, et al: A tissue level tolerance criterion for living brain developed with an in vitro model of traumatic mechanical loading. SAE Technical paper, 2003.
14. Giudice JS, Zeng W, Wu T, Alshareef A, Shedd DF, Panzer MB: An analytical review of the numerical methods used for finite element modeling of traumatic brain injury. Ann Biomed Eng 2019; 47(9): 1855–72.
15. Carlsen RW, Fawzi AL, Wan Y, Kesari H, Franck C: A quantitative relationship between rotational head kinematics and brain tissue strain from a 2-D parametric finite element analysis. Brain Multiphys 2021; 2: 100024–38.
16. Taylor PA, Ludwigsen JS, Ford CC, Vakhtin AA: *Verification and Validation of Simulation Framework for Analysis of Traumatic Brain Injury*. Sandia National Lab (SNL-NM); 2018.
17. Terpsma RJ, Hovey CB: *Blunt Impact Brain Injury Using Cellular Injury Criterion*. Sandia National Lab (SNL-NM); 2020.
18. Merewether MT, Treweek B, Wagman EB, et al: *Sierra/SolidMechanics 4.58 User's Guide*. Sandia National Lab (SNL-NM); 2020.
19. Haniff S, Taylor PA: In silico investigation of blast-induced intracranial fluid cavitation as it potentially leads to traumatic brain injury. Shock Waves 2017; 27(6): 929–45.
20. Taylor PA, Ludwigsen JS, Ford CC: Investigation of blast-induced traumatic brain injury. Brain Inj 2014; 28(7): 879–95.
21. Taylor PA, Ford CC: Simulation of blast-induced early-time intracranial wave physics leading to traumatic brain injury. J Biomech Eng 2009; 131(6): 061007–1–11.
22. Vakhtin AA, Calhoun VD, Jung RE, Prestopnik JL, Taylor PA, Ford CC: Changes in intrinsic functional brain networks following blast-induced mild traumatic brain injury. Brain Inj 2013; 27(11): 1304–10.
23. Taylor PA, Ludwigsen JS, Ford CC, Vakhtin AA: *Simulation of blast-induced early-time intracranial wave physics leading to traumatic brain injury and its mitigation by various helmet designs*. Sandia National Lab (SNL-NM); 2012.
24. Kleiven S: Predictors for traumatic brain injuries evaluated through accident reconstructions. Stapp Car Crash J 2007; 51: 81–114.
25. Zhang L, Yang KH, King AI: A proposed injury threshold for mild traumatic brain injury. J Biomech Eng 2004; 126(2): 226–36.
26. Geddes DM, Cargill RS, LaPlaca MC: Mechanical stretch to neurons results in a strain rate and magnitude-dependent increase in plasma membrane permeability. J Neurotrauma 2003; 20(10): 1039–49.
27. Takhounts EG, Eppinger RH, Campbell JQ, Tannous RE, Power ED, Shook LS: On the development of the SIMon finite element head model. SAE Technical paper, 2003.
28. Deck C, Willinger R: Improved head injury criteria based on head FE model. Int J Crashworthiness 2008; 13(6): 667–78.
29. Bain AC, Meaney DF: Tissue-level thresholds for axonal damage in an experimental model of central nervous system white matter injury. J Biomech Eng 2000; 122(6): 615–22.
30. Moss WC, King MJ: *Impact Response of US Army and National Football League Helmet Pad Systems*. Lawrence Livermore National Lab; 2011.
31. Aare M, Kleiven S: Evaluation of head response to ballistic helmet impacts using the finite element method. Int J Impact Eng 2007; 34(3): 596–608.
32. Begonia M, Rooks T, Pintar FA, Yoganandan N: Development of a methodology for simulating complex head impacts with the advanced combat helmet. Mil Med 2019; 184(Supplement_1): 237–44.
33. McIlwain H: Biochemistry and the central nervous system. 1st UK ed. Churchill; 1955: 272. ASIN: B0000CJ869.
34. Kleiven S: Influence of impact direction on the human head in prediction of subdural hematoma. J Neurotrauma 2003; 20(4): 365–79.
35. McIntosh AS, Lai A, Schilter E: Bicycle helmets: head impact dynamics in helmeted and unhelmeted oblique impact tests. Traffic Inj Prev 2013; 14(5): 501–8.
36. Post A, Hoshizaki TB, Gilchrist MD, Brien S, Cusimano M, Marshall S: Traumatic brain injuries: the influence of the direction of impact. Neurosurgery 2015; 76(1): 81–91.
37. Abel JM, Gennarelli TA, Segawa H: Incidence and severity of cerebral concussion in the rhesus monkey following sagittal plane angular acceleration. SAE Trans 1978; 87(4): 3144–50. Published online.
38. Miller LE, Urban JE, Davenport EM, et al: Brain strain: computational model-based metrics for head impact exposure and injury correlation. Ann Biomed Eng 2021; 49(3): 1083–96.
39. Carlsen RW, Daphalapurkar NP: The importance of structural anisotropy in computational models of traumatic brain injury. Front Neurol 2015; 6: 28.
40. Schmithorst VJ, Wilke M, Dardzinski BJ, Holland SK: Correlation of white matter diffusivity and anisotropy with age during childhood and adolescence: a cross-sectional diffusion-tensor MR imaging study. Radiology 2002; 222(1): 212–8.